Research

Authors for correspondence:
A. H. van Heteren
e-mail: vanheteren@snsb.de
S. Wroe
e-mail: swroe@une.edu.au

THE ROYAL SOCIETY
PUBLISHING

New Zealand's extinct giant raptor (*Hieraaetus moorei*) killed like an eagle, ate like a condor

A. H. van Heteren[1,2,3,4], S. Wroe[4], L. R. Tsang[4,5], D. R. Mitchell[4,6], P. Ross[7], J. A. Ledogar[8], M. R. G. Attard[4,9,10], D. Sustaita[11], P. Clausen[7], R. P. Scofield[12] and G. Sansalone[4]

[1]Sektion Mammalogie, Zoologische Staatssammlung München - Staatliche Naturwissenschaftliche Sammlungen Bayerns, Münchhausenstraße 21, 81247 Munich, Germany
[2]GeoBio-Center, Ludwig-Maximilians-Universität München, Richard-Wagner-Straße 10, 80333 Munich, Germany
[3]Department Biologie II, Ludwig-Maximilians-Universität München, Großhaderner Straße 2, 82152 Planegg-Martinsried, Germany
[4]School of Environmental and Rural Science, University of New England, Earth Sciences Building, NSW 2351 Armidale, Australia
[5]Ornithology Collection, Australian Museum Research Institute, 1 William Street, Sydney, Australia
[6]College of Science and Engineering, Flinders University, SA 5042 Adelaide, Australia
[7]School of Engineering, University of Newcastle, NSW 2308 Newcastle, Australia
[8]Department of Evolutionary Anthropology, Duke University, Durham, NC 27798, USA
[9]School of Engineering and Innovation, Open University: Milton Keynes, Buckinghamshire, UK
[10]Department of Biological Sciences, Royal Holloway University of London, Egham, Surrey TW20 0EX, UK
[11]Department of Biological Sciences, California State University San Marcos, 333 S. Twin Oaks Valley Rd., San Marcos, CA 92096, USA
[12]Natural History, Canterbury Museum, Rolleston Avenue, 8013 Christchurch, New Zealand

AHvH, 0000-0003-1018-7991; SW, 0000-0002-6365-5915; DRM, 0000-0003-1495-4879;
MRGA, 0000-0002-8509-3677; DS, 0000-0001-9932-909X; RPS, 0000-0002-7510-6980

The extinct Haast's eagle or harpagornis (*Hieraaetus moorei*) is the largest known eagle. Historically, it was first considered a predator, then a scavenger, but most recent authors have favoured an active hunting ecology. However, the veracity of proposed similarities to carrion feeders has not been thoroughly tested. To infer feeding capability and behaviour in harpagornis, we used geometric morphometric and finite-element analyses to assess the shape and biomechanical strength of its neurocranium, beak and talons in comparison to five extant scavenging and predatory birds. The neurocranium of harpagornis is vulture-like in shape whereas its beak is eagle-like. The mechanical performance of harpagornis is closer to extant eagles under biting loads but is closest to the Andean condor (*Vultur gryphus*) under extrinsic loads simulating prey capture and killing. The talons, however, are eagle-like and even for a bird of its size, able to withstand extremely high loads. Results are consistent with the proposition that, unlike living eagles, harpagornis habitually killed prey larger than itself, then applied feeding methods typical of vultures to feed on the large carcasses. Decoupling of the relationship between neurocranium and beak shape may have been linked to rapid evolution.

1. Introduction

Accipitrid birds of prey (Aves: Accipitriformes) are a diverse group composed of eagles, kites and Old World vultures. Raptorial birds predominately feed on animals and have specific prey preferences. Some raptorial species specialize on mammals, reptiles, amphibians, fish, other birds or carrion, whereas others are generalists, feeding on a variety of prey, including invertebrates [1]. Different feeding preferences among raptorial birds require different hunting strategies and consequently divergently adapted morphological structures [1–3]. For

example, skull shape and morphology of the cervical musculature in raptors are thought to correlate with diet and feeding behaviour [1,4,5], as well as the feet [6,7] and talons [8]. By contrast, the feeding behaviours of scavengers are classified as rippers, which feed primarily on the tough skin and hide of a carcass, gulpers, which feed primarily on the softer viscera, or scrappers, which feed primarily on smaller scraps [4]. Vultures are the only obligate scavenging vertebrates [9,10] and can feed on decaying animal carcasses without compromising their health [11–13]. The diversity in feeding ecologies among extant birds of prey may be used to reconstruct feeding and dietary preferences of closely related extinct taxa based on morphometric and mechanical similarities [1].

New Zealand's iconic harpagornis or Haast's eagle (*Hieraaetus moorei*) [14–16] is an extinct eagle that weighed up to 15 kg [17], approximately 30–40% heavier than the largest living eagle (the harpy eagle, *Harpia harpyja*) [16]. Once thought to be descended from Australia's largest extant eagle, the wedge-tailed eagle (*Aquila audax*), DNA analysis has demonstrated that its closest living relative is in fact one of the world's smallest eagles, another Australian raptor, the little eagle (*Hieraaetus morphnoides*) [16]. *Hieraaetus moorei* was more than an order of magnitude heavier than the *Hie. morphnoides* and represents an extraordinary example of rapid evolution within less than 2 million years [16].

Hieraaetus moorei was first described as an active predator [18], but Haast himself later noted that its beak exhibited vulturine features [19], as have more recent authors [3,17] who also observed vulture-like similarities in beak shape, based on two-dimensional morphometrics, as well as the presence of bone scrolls around the nostrils. Through much of the twentieth century, the argument that it was largely a carrion feeder was widely held [20]. However, most of the more recent studies have supported the predator hypothesis [21–23].

In recent years, the argument that the giant eagle was a predator has been based on interpretations of its nervous system, among other features. Well-developed hind limb innervation indicates that its talons were sensitive and powerful enough to grapple with live prey, even though it lacks some visual, olfactory and vestibular features that are common to many vultures [23]. The hunting hypothesis has been further supported by two-dimensional shape analysis and qualitative studies that have shown overall similarity in body shape and talon morphology with large extant eagles [17]. The size of *Hie. moorei* has fuelled speculation that they may have been able to kill moa of adult size (200 kg) [23] and is supported by perforations in the pelvic bones of moa thought to have been inflicted by *Hie. moorei* [17,24]. Although a largely predacious ecology is now widely accepted, the validity of conflicting indications given by beak, neurocranium and talon data has not yet been tested using more powerful three-dimensional shape analyses, nor have the mechanical consequences proposed for these features been tested by computation simulation.

It has long been argued that the shape of bird beaks is driven by natural selection for specific feeding behaviours in at least some bird taxa [25]. Across avian taxa, diet explains only 12% of the variation in bill shape [26], and among raptors, the shape of the cranium is a better predictor of feeding behaviour than the shape of the beak [1]. Furthermore, beak and cranial shapes are tightly integrated and largely controlled by allometry [27]. This suggests that the capacity of

beak shape to respond independently to natural selection is highly constrained and correlated largely to changes in body size.

The relationship between talon morphology and diet in raptors is less equivocal [1,28]. Predacious raptors have evolved hypertrophied talons on digits I and II to retain struggling prey [28]. Ecomorphological differences in talon : toe length ratios have been observed among some dietary specialists [29,30], such as the high talon : toe ratios of the *Aqu. audax* and white-bellied sea eagle (*Haliaeetus leucogaster*), which specialize in prey that are large and/or difficult to capture [28]. General differences in claw size (claw radius) and shape (claw angle and curvature) among birds reflect specific aspects of their ecology, with variable degrees of differentiation among large-scale functional groups, such as 'ground-dwelling' versus 'climbing' versus 'perching' birds [31,32]. In birds of prey, claw shape largely differs by order and family [29,30], but can also have important functional consequences [30,33]. Furthermore, talon shape and mechanical performance have evolved in direct response to relative prey size, without allometric or phylogenetic constraint [8].

Although several studies have addressed the functional morphology of skulls and feet among Accipitriformes [1,28–30,34], little is known about their load-bearing performance. Previous morphology-based interpretations of ecology for *Hie. moorei* have been based on two-dimensional shape analysis and qualitative inference [3,17]. Here, we use three-dimensional shape analysis (geometric morphometrics, GMM) and computer-based simulations of biomechanical performance (finite-element analysis, FEA) to compare the beak, neurocranium and talon of *Hie. moorei* to those of extant raptors, and thereby determine whether the shapes and mechanical performances of each are consistent with hunting or scavenging roles. We also test whether the evolution of beak shape in the world's largest eagle was tightly integrated with neurocranium shape and controlled by size, as is the case in other eagles.

2. Material and methods

(a) Shape analysis

Surface models of the skulls and talons were created in Mimics software (v. 16.0, Materialise NV, Belgium) for six species (table 1). Thirty-seven anatomical landmarks and 150 sliding semi-landmarks, placed equidistantly along with six homologous curves, were digitized onto the cranium (derived from [27]). Definitions and diagrams of anatomical landmarks and sliding semi-landmarks on the cranium are provided in the electronic supplementary material, table S1 and figure S1. On each talon, we digitized eight anatomical landmarks and 65 semi-landmarks placed equidistantly along the outer and inner curves of the ungual bone to capture its shape in three dimensions [8] using IDAV Landmark software (UC Davis) (electronic supplementary material, figure S2). The landmark coordinates were imported into R v. 4.0.4 [35,36] for further analyses. We performed generalized Procrustes analysis on all landmarks, implemented in the ProcSym() function from the R package 'Morpho' [36], to rotate, translate and scale landmark configurations to unit centroid size.

To visualize the multivariate ordination of the aligned Procrustes coordinates, we performed a principal component analysis (PCA). Phenograms describing cranium and talon shape relationships among the taxa were created by performing an unweighted pair group method with arithmetic mean (UPGMA)

Table 1. Basic information on the six species used in this study (references are in the electronic supplementary material). Bird art by Scott Partridge.

icon in the figures	Latin abbreviation	English name	model volume as proxy for mass (mm³)	foraging behaviour
	Hal. sphenurus	whistling kite	7070	active hunter, variety of small animals, but will also feed on carrion
	Hie. morphnoides	little eagle	11 865	active hunter, feeding on mammals and birds, can catch prey exceeding own body mass
	Aqu. audax	wedge-tailed eagle	24 037	active hunter, dietary generalist, feeding on mammals, birds and reptiles
	Hie. moorei	Haast's eagle	67 807	
	Aeg. monachus	cinereous vulture	64 489	obligate scavenger, ripper, medium-sized to large carcasses
	Vul. gryphus	Andean condor	31 891	obligate scavenger, gulper, medium-sized to large carcasses

on the Euclidean distance matrix of different sets of landmarks. The UPGMA is a simple distance-matrix method that uses sequential clustering to reconstruct phenetic similarities [37].

(b) Finite-element analysis

Precise details on protocols used for FEA are provided in the electronic supplementary material, but a summary is given here. Six major jaw-closing muscles were modelled for each of the six species included based on a digital dissection of a buzzard (*Buteo buteo*) [38]: *Pterygoideus dorsalis*, *Pterygoideus ventralis*, *Pseudotemporalis profundus*, *Pseudotemporalis superficialis*, *Adductor mandibulae externus profundus* and *Adductor mandibulae externus medialis/superficialis*. Volume meshes of each element were created in Mimics (v. 16.0) and 3-Matic (v. 8.0, Materialise). The models and the loaded muscle origin plates were imported into Strand7 (v. 2.4.6., Strand7 Pty Ltd., Sydney, Australia). One intrinsic loading case was used for the cranium to simulate bites driven solely by jaw musculature. Additionally, three extrinsic loading cases were analysed for the cranium, representing different behavioural strategies used in feeding or incapacitating prey: dorsoventral pull, lateral shake and pull back [39]. The force was applied to the tip of the beak. Detailed information on the models can be found in the electronic supplementary material. A dorsoventral pull simulates head depression towards the bird's body about a mediolateral axis perpendicular to the long axis of the cranium (i.e. pitch), a lateral shake simulates the head moving side-to-side about a dorsoventral axis perpendicular to the long axis of the cranium (i.e. yaw) and a pullback simulates the beak pulling the prey in line with the long axis of the cranium. For the talons,

two nodes to fix the bone in space were placed on either side of the flexor tubercle, the attachment site of the *Musculus flexor hallucis longus*. Intrinsic load cases were solved with calculated node forces applied in the negative z-axis direction to simulate the piercing action of the talon.

(c) Von Mises strain analysis

To allow a direct comparison of results between talon finite-element models (FEMs), and to further integrate strain and shape outputs from FEA with GMM, we followed previously published methodology and computed the mean von Mises (VM) strain values at the location of 21 selected landmarks [8]. The lower the VM strain values, the better adapted the talon is to sustain high pressure/loads during prey capture and restraint. Higher VM strain values indicate that the talon is less well adapted to deliver high-gripping forces. For the cranium, we computed the mean VM strain values from the four nearest tetrahedral elements (each element has four nodes) at the locations of the 37 homologous landmarks, which were also used in the shape analysis (red landmarks on electronic supplementary material, figure S1).

3. Results

(a) Shape analysis of the crania

PCA results for three-dimensional shape analysis of the crania (figure 1) revealed morphological differences among raptor species based on dietary mode. At the positive extreme
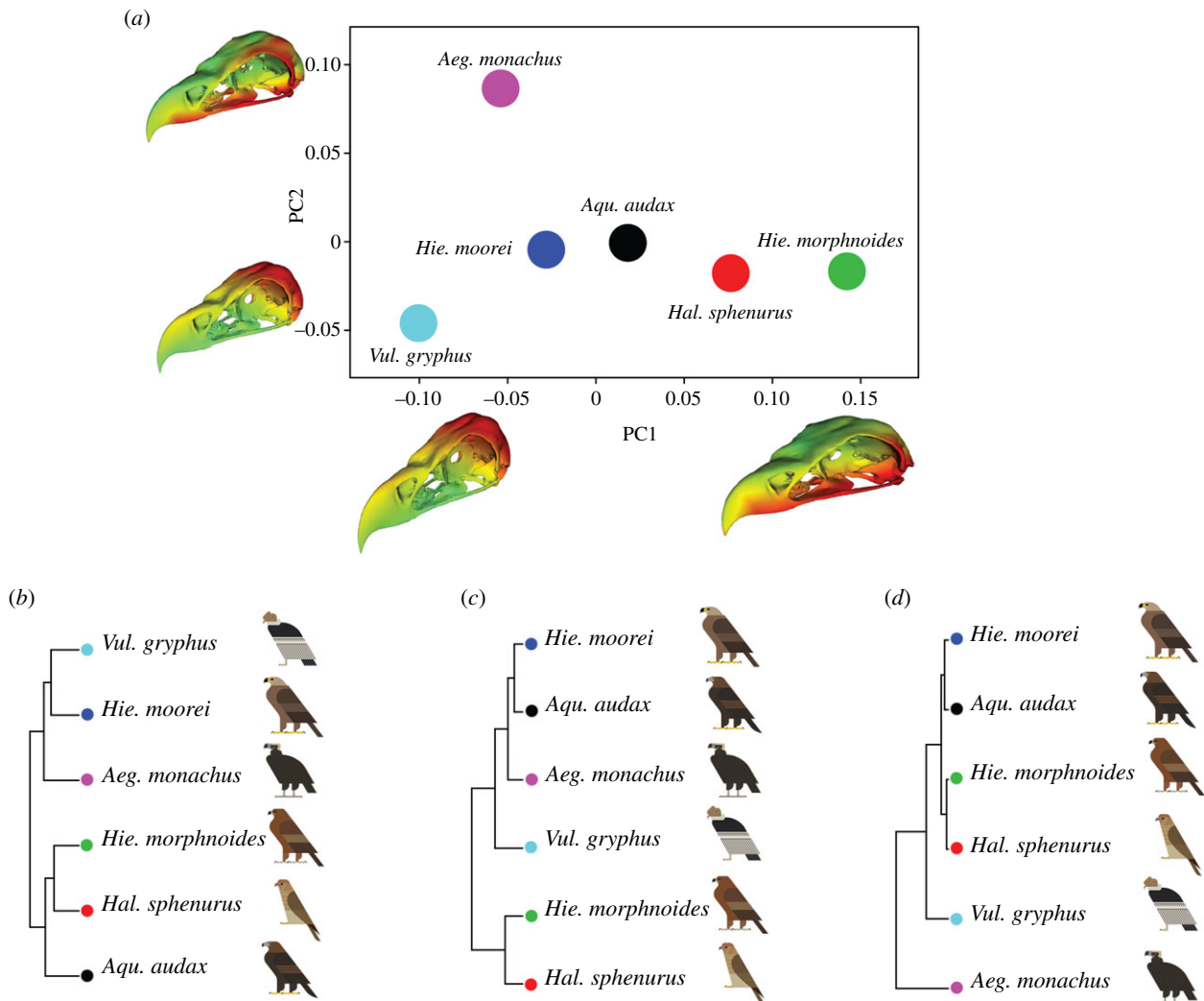
Figure 1. Three-dimensional cranial shape variation in Acciptriformes. (*a*) Scatterplot depicting the morphospace of six species of raptorial bird: *Aeg. monachus*, *Aqu. audax*, *Hie. moorei*, *Hie. morphnoides*, *Hal. sphenurus* and *Vul. gryphus*. Warped meshes refer to cranial shape in the extremes of the axes and the meshes heatmaps are based on euclidean distances: cooler colours (blue-green) indicate minor changes and warmer colours (orange-red) indicate major changes. (*b*) UPGMA performed on all PC scores (*c*) and on PC1 (*d*) and on PC2 scores. Bird art by Scott Partridge. (Online version in colour.)

of PC1 (38.4% of total variation), the cranium showed a shorter beak and a wider and flatter neurocranium, as exemplified by the smaller species, *Hal. sphenurus* and *Hie. morphnoides* (figure 1*a*). The larger species (*Aqu. audax*, *Hie. moorei* and *Vul. gryphus*) positioned on the lower PC1 extremes displayed a narrower neurocranium and a longer beak. PC2 (23.6%) separates the two vulture species, with *Aeg. monachus* (positive values) characterized by a wider neurocranium and a larger occipital condyle, whereas *Vul. gryphus* (negative values) had a narrower and taller neurocranium. The PC3 axis (16.7%) separated accipitrid birds of prey into two groups based on neurocranium width: vultures and *Hie. moorei* (negative PC3 values) had a taller and narrower neurocranium whereas other eagles and the kite (positive PC3 values) had a wider neurocranium (electronic supplementary material, figure S4).

UPGMA is a simple hierarchical clustering method based on dissimilarity matrices [38]. UPGMA (figure 1*b*) conducted on the full set of shape variables revealed close similarities between *Hie. moorei* and both vultures. However, UPGMAs performed on PC1 and PC2 scored separately shows that *Hie. moorei* was most like *Aqu. audax*. This result for separate PC1 scores (figure 1) was largely explained by similarity in beak shape between these two large eagle species.

UPGMA based on PC2 (figure 1*b*) highlighted differences between the two extant carrion feeders (*Vul. gryphus* and *Aeg. monachus*), at least in part explained by phylogeny. UPGMA on PC3 (electronic supplementary material, figure S5) showed that *Hie. moorei* is more vulture-like regarding the overall shape of the cranium, largely due to similarities in the orientation of the foramen magnum and relative cranial width.

(b) Finite-element analysis of the crania
Mean VM strain values for each of the four load cases are in table 2. Visual outputs of strain in the cranium for all load cases are shown in figure 2 and associated UPGMA phylogenetic tree constructions are shown in figure 2 (see electronic supplementary material, figures S6–S9 and table S2 for further details). In the intrinsic (biting) load case, mean strain was markedly less in *Hie. moorei* than in all other taxa, although closest to *Aeg. monachus*. Strain values were similar among the remaining species, except *Hal. sphenurus* in which strain values were high; UPGMA results were not consistent with these mean values but showed high similarity of *Hie. moorei* with *Aqu. audax* and *Hie. morphnoides* (figure 2). Unlike both vultures, but like *Aqu. audax*, *Hie. moorei* displayed extremely low strains mid-beak (figure 2).
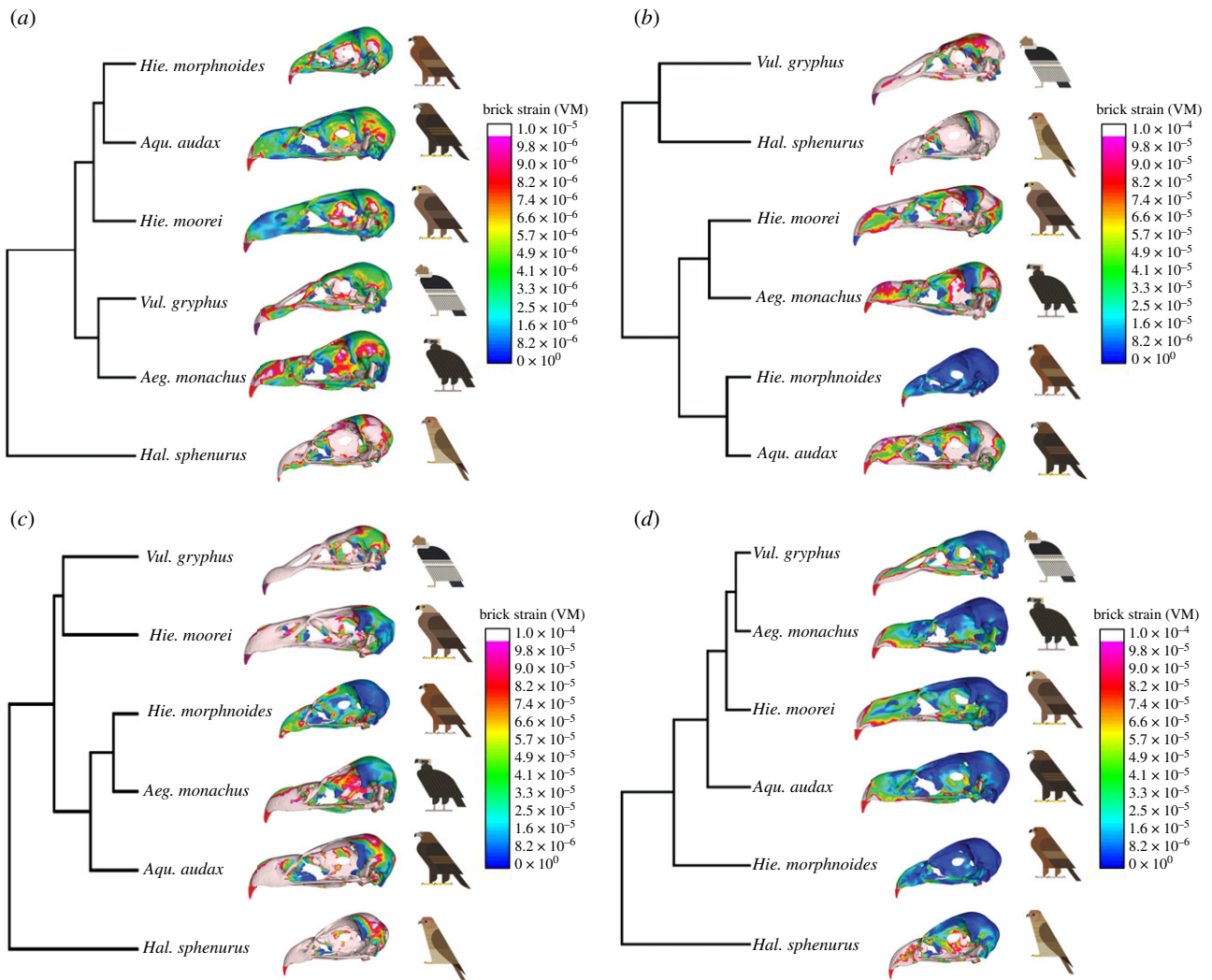
Figure 2. VM strain contour plots of the crania in the intrinsic, dorsoventral, lateral shake and pullback load cases in lateral view and UPGMAs performed on PC scores of VM strains collected at specific landmarks for each of the considered load cases: (*a*) intrinsic, (*b*) dorsoventral, (*c*) lateral shake and (*d*) pullback. Models are not to scale. Bird art by Scott Partridge. (Online version in colour.)

Table 2. Mean VM strains for each of the considered cranial loading cases and the talon. Cranial loading cases consisted of one intrinsic load and three extrinsic (dorsoventral, lateral and pullback) loads.

species	intrinsic	dorsoventral pull	lateral shake	pullback	talon
Hal. sphenurus	14.15×10^{-5}	21.851×10^{-4}	15.372×10^{-4}	10.944×10^{-4}	5.2887
Hie. morphnoides	5.41×10^{-5}	0.1339×10^{-4}	3.149×10^{-4}	7.036×10^{-4}	5.5069
Aqu. audax	6.70×10^{-5}	0.718×10^{-4}	5.923×10^{-4}	5.518×10^{-4}	3.3678
Hie. moorei	2.58×10^{-5}	10.563×10^{-4}	10.180×10^{-4}	3.648×10^{-4}	1.6324
Aeg. monachus	5.07×10^{-5}	0.7449×10^{-4}	2.838×10^{-4}	2.876×10^{-4}	7.6279
Vul. gryphus	6.64×10^{-5}	12.848×10^{-4}	10.596×10^{-4}	3.481×10^{-4}	6.7893

For the dorsoventral load, mean strain was intermediate in *Hie. moorei*, falling between that recorded for *Vul. gryphus* and *Aeg. monachus* (table 2). The values for *Aeg. monachus* were also intermediate and values for *Aqu. audax* and *Hie. morphnoides* were very low, especially for *Hie. morphnoides*. *Haliastur sphenurus* experienced the highest strain. These results were consistent with those of the UPGMA (figure 2). The strain pattern in *Hie. moorei* was most like that of *Aqu. audax*, with a band of high strains across the braincase and a spot of low strains on the side of the beak (figure 2). In

the lateral shake, mean strain in the cranium of *Hie. moorei* was relatively high and similar to that of *Vul. gryphus* (figure 2 and table 2). The two extant eagle species recorded low strains, although the lowest were in *Aeg. monachus*. *Haliastur sphenurus* recorded the highest strain. Under the pullback simulation, *Hie. moorei* showed relatively low strain, comparable to that of *Vul. gryphus* and the other scavenger, *Aeg. monachus* (table 2). *Aquila audax* and *Hie. morphnoides* recorded higher strains, but again the highest was in *Hal. sphenurus*. These results are also reflected in the UPGMA (figure 2).
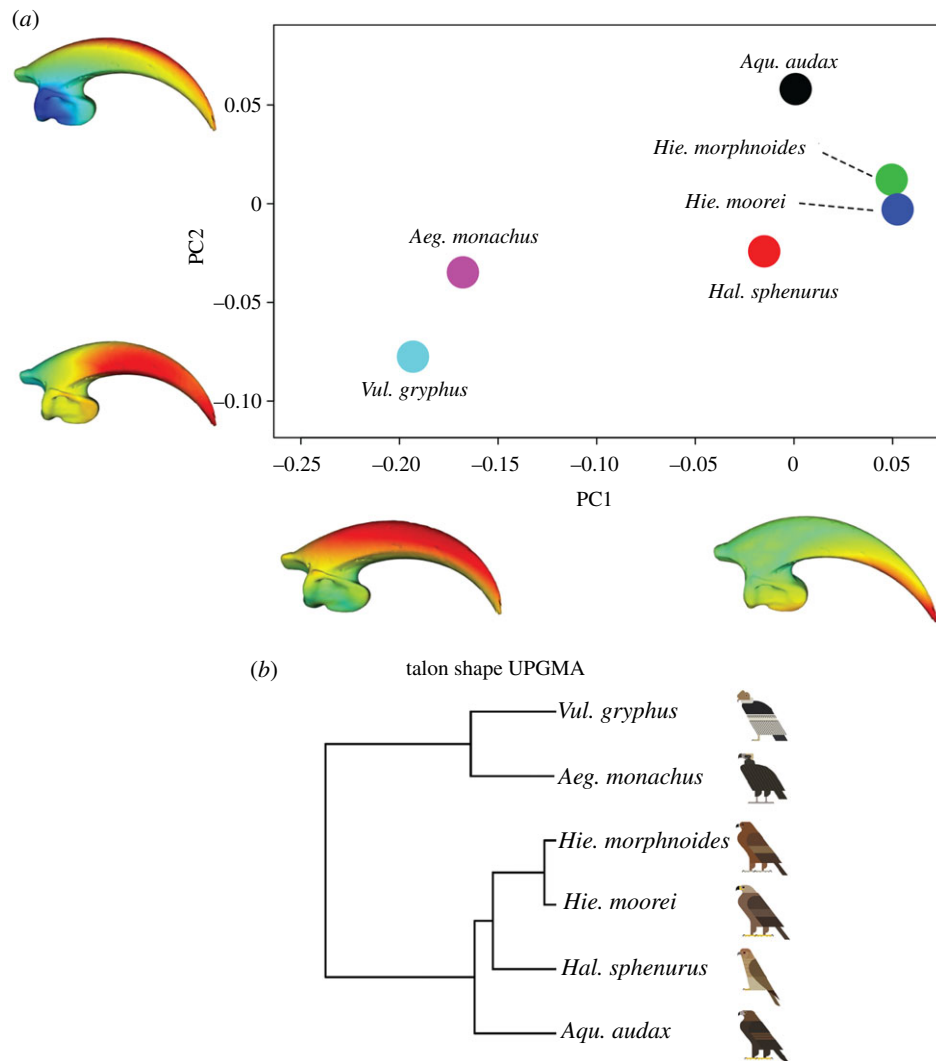
Figure 3. Three-dimensional talon shape variation in Acciptriformes. *(a)* Scatterplot depicting the morphospace of six species of raptorial bird: *Aeg. monachus*, *Aqu. audax*, *Hie. moorei*, *Hie. morphnoides*, *Hal. sphenurus* and *Vul. gryphus*. Warped meshes refer to talon shape in the extremes of the axes and the meshes heatmaps are based on Euclidean distances: cooler colours (blue-green) indicate minor changes and warmer colours (orange-red) indicate major changes. *(b)* UPGMA performed on the entire shape based on all PC scores. Bird art by Scott Partridge. (Online version in colour.)

(c) Shape analysis of the talons

The first two PCs (52.5% and 25.1%, respectively, of total variation) for shape analysis of the talons clearly separated the vultures from the other raptors (figure 3). Vultures had a shorter and blunter talon with decreased curvature and reduced ungual articular surface, whereas the raptorial taxa were characterized by a more curved, longer and pointed ungual shaft and larger, more robust ungual articular face (figure 3*a*). There was no allometric scaling in the talons. UPGMA performed on all shape variables (the whole set of PC scores) showed that *Hie. moorei* was most like *Hie. morphnoides* (figure 3*b*).

(d) Finite-element analysis of the talons

Mean strain data (table 2) and UPGMA of strain results for the talons of six raptor species (figure 4) showed that *Hie. moorei* was most like *Aqu. audax*, the largest extant eagle in our analysis. However, mean strain data were considerably lower in *Hie. moorei* than in any of the other raptors. *Hieraaetus moorei* showed consistently lower strain values in the ventral region of the inner curvature, on the outer curvature and on the flexor tubercle when compared to *Aqu. audax*. *Hieraaetus*
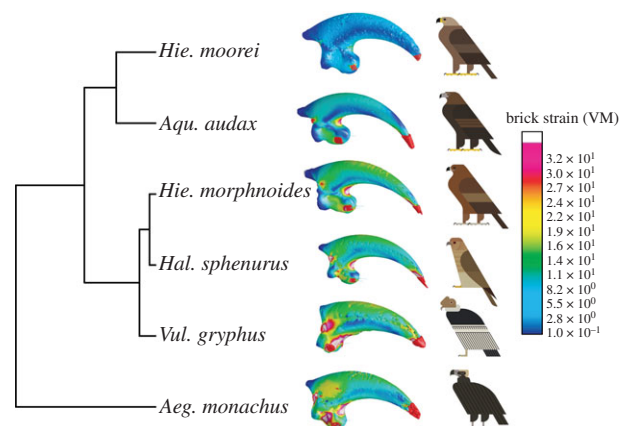

Figure 4. UPGMA performed on PC scores of VM strains collected at specific landmarks on the talons and associated solved FEMs. Models are not to scale. Bird art by Scott Partridge. (Online version in colour.)

morphnoides and *Hal. sphenurus* showed intermediate strain values, whereas the two carrion feeders displayed the highest strain.

4. Discussion

Whether *Hie. moorei* was primarily a scavenger or an active predator has been a subject of long-running debate. Although the argument that it was predacious has prevailed, until recent times, morphology-based hypotheses have largely been deduced through qualitative interpretations and comparisons, as well as limited two-dimensional shape analyses [17]. Additionally, no analyses of mechanical performance have been conducted on preserved skeletal material that might support or refute either hypothesis. Results of our combined analyses reveal a novel mosaic of morphological and biomechanical features attributable to the cranium of *Hie. moorei*. Regarding shape, its beak is eagle-like but its neurocranium is closest to that of the two carrion feeders, *Vul. gryphus* in particular. This contradicts interpretations based on two-dimensional analyses that the closest similarities between *Hie. moorei* and vultures were evident in the beak [17].

Hieraaetus moorei was also characterized by a combination of eagle-like and vulture-like features with respect to the mechanical performance of the cranium. Under the intrinsic load, mean strain in *Hie. moorei* was considerably lower than in any other taxon, but closest to that of eagles. This suggests a capacity to withstand loads generated by a particularly powerful bite for its size. High mean strains recorded in *Vul. gryphus*, *Hal. sphenurus* and *Hie. moorei* for dorsoventral pulling suggest that these species are not well adapted for this behaviour. Similarly, high mean strain for *Hie. moorei* under the lateral shaking simulation indicates that this species was poorly adapted to perform this behaviour relative to extant eagles and again was closest to the carrion feeding *Vul. gryphus*. Interestingly, the other carrion feeder, the *Aeg. monachus*, records very low strain for the lateral shake. Under the pullback loading, *Hie. moorei* and the two scavengers all perform better than the remaining taxa and the giant eagle was again closest to *Vul. gryphus*, which is consistent with feeding observations and functional anatomy of vultures [1,5].

The interpretation of both shape analysis and FEA results of the talon show that *Hie. moorei* is unambiguously eagle-like (showing similarities with *Aqu. audax*) and capable of resisting particularly high loadings. Interestingly, *Hie. moorei* showed the closest morphological similarities with the phylogenetically closest *Hie. morphnoides*. This is in agreement with the results provided by Tsang *et al.* [8], which showed no significant allometric signal in talon shape. In the case of *Hie. moorei*, the increase in size of the talon probably reflects the adaptation to killing very large prey relative to the body mass of the bird, but in this case, could also be driven by phylogenetic inertia.

Overall, the beak of *Hie. moorei* is eagle-like and its neurocranium vulture-like, bearing the closest resemblance to *Vul. gryphus* among the two scavengers. Results of FEA simulations of feeding behaviour show *Hie. moorei* performs very well under the biting simulation, but poorly under dorsoventral and lateral loadings. Under the pullback load, *Hie. moorei* outperforms the other two eagles and is again closest to *Vul. gryphus*. Thus, with respect to the four FEA simulations, it is closest to the eagles in the capacity to deliver a powerful bite, but closest to the obligate carrion feeder *Vul. gryphus* in all others. Its talon on the other hand is eagle-like in every respect and able to withstand high forces, even for its large body mass.

How then to interpret this unique combination of characters in *Hie. moorei*? Talons are the primary killing tools of most raptors, except falcons; however, their beak may be used to finish a kill [1,30]. We propose that biting may have been more important in delivering the kill for *Hie. moorei* than is typical among extant eagles. With respect to the extrinsic FEA, we first note that there is a clear difference between the two known carrion feeders included in the analyses. *Aegypius monachus* was able to withstand high lateral loadings, whereas both *Hie. moorei* and *Vul. gryphus* performed poorly in this regard. This is consistent with the classification of *Aeg. monachus* as a ripper of flesh that favours the tough skin and meat of large mammal carcasses [4], possibly with strong lateral forces as well as powerful biting. *Aegypius monachus* is a large and aggressive vulture that dominates other avian scavengers when fights occur over a carcass [40,41]. By contrast, *Vul. gryphus* is a 'gulper' that focuses on the softer internal organs [4]. Our findings of more vulture-like features in the extrinsic FEAs, therefore, are most consistent with the proposition that *Hie. moorei* may have preferentially targeted the high nutrient viscera of its prey that are also favoured by most carrion-feeding raptors [42].

This mix of morphologies and mechanical behaviours reminiscent of obligate carrion feeders, as well as predacious eagles, may be the result of a unique combination of selective pressures. Vultures generally feed on animals much larger than themselves, but eagles typically kill and eat relatively small prey [1]. Taphonomic evidence leaves little doubt that *Hie. moorei* killed and fed on moa, including the largest, *Dinornis*, which could weigh over 200 kg [43–45]. Even the smallest of moa species (little bush moa, *Anomalopteryx didiformis*; approximately 30 kg [46]) was larger than *Hie. moorei*. *Hieraaetus moorei* probably inhabited open plains [23], as did many of its prey species [44]. Its vision was evidently not particularly acute [23], but without competition, this was probably not under strong selection. *Hieraaetus moorei* used a flapping flight [17], suggesting flight occurred over relatively short distances. Together the evidence suggests that *Hie. moorei* could have swooped down from trees or cliffs at short distances to catch and kill its prey. Our results are largely consistent with the proposition that *Hie. moorei* habitually killed particularly large prey in a typically eagle-like fashion using its powerful talons, but then applied feeding techniques common to vultures that eat from the carcasses of species much larger than themselves. Bird skin is typically less tough than that of mammals [1,48], so *Hie. moorei* was able to open the carcasses itself. It is notable that *Hie. moorei* is less well adapted to eating hard tissues, such as tendons, than *Aegypius* [40], but probably preferred viscera and muscles, like *Vultur* [48].

Our proposal that *Hie. moorei* favoured the internal organs of its prey leads to the possibility that, as well as vulture-like nostril scrolls [17] and vulture-like feeding mechanics, like most vultures, its head and neck were featherless. This proposition is also consistent with a Maori rock art depiction of what is thought to be a *Hie. moorei*, in the Cave of the Eagle at Craigmore Station, South Island (figure 5). The raptorial bird has a dark-coloured body, but the head and neck remain uncoloured.

Rapid evolution has been demonstrated for insular taxa [49]. We further postulate that the increase in modularity between the neurocranium and the beak in *Hie. moorei* may have facilitated the rapid evolution of *Hie. moorei* from its common ancestor with *Hie. morphnoides*. In conclusion, *Hie. moorei* is characterized

Figure 5. At Craigmore Station, inland Timaru, the Cave of the Eagle shows a painting of *Hie. moorei* with a dark-coloured body, but an uncoloured head. Photographed by Gerard Hindmarsh. (Online version in colour.)

by a unique mosaic of eagle and vulture-like features that probably evolved in response to highly demanding selective pressures to routinely hunt and eat particularly large prey.

References

1. Hertel F. 1995 Ecomorphological indicators of feeding behavior in recent and fossil raptors. *Auk* **112**, 890–903. (doi:10.2307/4089021)

2. Roulin A, Wink M. 2004 Predator-prey relationships and the evolution of colour polymorphism: a comparative analysis in diurnal raptors. *Biol. J. Linn. Soc.* **81**, 565–578. (doi:10.1111/j.1095-8312.2004.00308.x)

3. Pecsics T, Laczi M, Nagy G, Kondor T, Csörgő T. 2019 Analysis of skull morphometric characters in diurnal raptors (Accipitriformes and Falconiformes). *Ornis Hungarica* **27**, 117–131. (doi:10.2478/orhu-2019-0008)

4. Hertel F. 1994 Diversity in body size and feeding morphology within past and present vulture assemblages. *Ecology* **75**, 1074–1084. (doi:10.2307/1939431)

5. Böhmer C, Prevoteau J, Duriez O, Abourachid A. 2020 Gulper, ripper and scrapper: anatomy of the neck in three species of vultures. *J. Anat.* **236**, 701–723. (doi:10.1111/joa.13129)

6. Tsang LR, McDonald PG. 2018 A comparative study of avian pes morphotypes, and the functional implications of Australian raptor pedal flexibility. *Emu—Austral. Ornithol.* **119**, 14–24. (doi:10.1080/01584197.2018.1483203)

7. Tsang LR, Wilson LAB, McDonald PG. 2019 Comparing the toepads of Australian diurnal and nocturnal raptors with non-predatory taxa: insights into functional morphology. *J. Morphol.* **280**, 1632. (doi:10.1002/jmor.21057)

8. Tsang LR, Wilson LAB, Ledogar J, Wroe S, Attard M, Sansalone G. 2019 Raptor talon shape and biomechanical performance are controlled by relative prey size but not by allometry. *Sci. Rep.* **9**, 7076. (doi:10.1038/s41598-019-43654-0)

9. Donázar JA. 1993 *Los buitres ibéricos: biología y conservación*, 1st edn, Madrid, Spain: JM Reyero.

10. Campbell MON. 2015 *Vultures: their evolution, ecology and conservation*, 1st edn. Boca Raton, FL: CRC Press.

11. Roggenbuck M *et al.* 2014 The microbiome of New World vultures. *Nat. Commun.* **5**, 5498. (doi:10.1038/ncomms6498)

12. Waite D, Taylor M. 2015 Exploring the avian gut microbiota: current trends and future directions. *Front. Microbiol.* **6**, 673. (doi:10.3389/fmicb.2015.00673)

13. Blumstein DT, Rangchi TN, Briggs T, De Andrade FS, Natterson-Horowitz B. 2017 A systematic review of carrion eaters' adaptations to avoid sickness. *J. Wildl Dis.* **53**, 577–581. (doi:10.7589/2016-07-162)

14. Lerner H *et al.* 2017 Phylogeny and new taxonomy of the Booted Eagles (Accipitriformes: Aquilinae). *Zootaxa* **4216**, 301–320. (doi:10.11646/zootaxa.4216.4.1)

15. Mindell DP, Fuchs J, Johnson JA. 2018 Phylogeny, taxonomy, and geographic diversity of diurnal raptors: Falconiformes, Accipitriformes, and Cathartiformes. In *Birds of prey: biology and conservation in the XXI century* (eds JH Sarasola, JM Grande, JJ Negro), pp. 3–32. Cham, Switzerland: Springer International Publishing.

16. Bunce M, Szulkin M, Lerner HRL, Barnes I, Shapiro B, Cooper A, Holdaway RN. 2005 Ancient DNA provides new insights into the evolutionary history of New Zealand's extinct giant eagle. *PLoS Biol.* **3**, e9. (doi:10.1371/journal.pbio.0030009)

17. Holdaway RN. 1991 Systematics and palaeobiology of Haast's eagle. PhD thesis, University of Canterbury, Canterbury.

18. Haast J. 1872 Notes on *Harpagornis moorei*, an extinct gigantic bird of prey, containing descriptions of femur, ungual phalanges, and rib. *Trans. Proc. New Zealand Institute* **4**, 192–196.

19. Haast J. 1880 On Harpagornis (third paper). *Trans. Proc. R. Soc. New Zealand* **13**, 232–234.

20. Trotter MM, McCulloch B. 1984 Moas, men, and middens. In *Quaternary extinctions: a prehistoric revolution* (eds PS Martin, RG Klein), pp. 708–727. Tucson, AZ: University of Arizona Press.

21. Brathwaite DH. 1992 Notes on the weight, flying ability, habitat, and prey of Haast's eagle (*Harpagornis moorei*). *Notornis* **39**, 239–247.

22. Holdaway RN. 1989 New Zealand's pre-human avifauna and its vulnerability. *New Zealand J. Ecol.* **12**, 11–25.

23. Scofield RP, Ashwell KWS. 2009 Rapid somatic expansion causes the brain to lag behind: the case of the brain and behavior of New Zealand's Haast's eagle (*Harpagornis moorei*). *J. Vertebr. Paleontol.* **29**, 637–649. (doi:10.1671/039.029.0325)

24. Holdaway R, Worthy T. 2008 The Late Quaternary avifauna. In *The natural history of Canterbury* (eds MJ Winterbourn, GA Knox, CJ Burrows, ID Marsden), pp. 445–492, 3rd edn. Christchurch, New Zealand: Canterbury University Press and Manaaki Whenua Press.

25. Grant BR, Grant PR. 1993 Evolution of Darwin's finches caused by a rare climatic event. *Proc. R. Soc. Lond. Ser. B* **251**, 111. (doi:10.1098/rspb.1993.0016)

26. Navalón G, Bright JA, Marugán-Lobón J, Rayfield EJ. 2019 The evolutionary relationship among beak shape, mechanical advantage, and feeding ecology in modern birds. *Evolution* **73**, 422–435. (doi:10.1111/evo.13655)

27. Bright JA, Marugán-Lobón J, Cobb SN, Rayfield EJ. 2016 The shapes of bird beaks are highly controlled by nondietary factors. *Proc. Natl Acad. Sci. USA* **113**, 5352–5357. (doi:10.1073/pnas.1602683113)

28. Einoder LD, Richardson AMM. 2007 Aspects of the hindlimb morphology of some Australian birds of prey: a comparative and quantitative study. *Auk* **124**, 773–788. (doi:10.1642/0004-8038(2007)124[773:AOTHMO]2.0.CO;2)

29. Csermely D, Rossi O. 2006 Bird claws and bird of prey talons. Where is the difference? *Italian J. Zool.* **73**, 43–53. (doi:10.1080/11250000500502368)

30. Fowler DW, Freedman EA, Scannella JB. 2009 Predatory functional morphology in raptors: interdigital variation in talon size is related to prey restraint and immobilisation technique. *PLoS ONE* **4**, e7999. (doi:10.1371/journal.pone.0007999)

31. Pike AVL, Maitland DP. 2006 Scaling of bird claws. *J. Zool.* **262**, 73–81. (doi:10.1017/S0952836903004382)

32. Birn-Jeffery AV, Miller CE, Naish D, Rayfield EJ, Hone DWE. 2012 Pedal claw curvature in birds, lizards and Mesozoic Dinosaurs: complicated categories and compensating for mass-specific and phylogenetic control. *PLoS ONE* **7**, e50555. (doi:10.1371/journal.pone.0050555)

33. Fowler DW, Freedman EA, Scannella JB, Kambic RE. 2011 The predatory ecology of *Deinonychus* and the origin of flapping in birds. *PLoS ONE* **6**, e28964. (doi:10.1371/journal.pone.0028964)

34. Hertel F. 1992 Morphological diversity of past and present New World vultures. In *Papers in avian paleontology honoring Pierce Brodkorb* (eds KEJ Campbell). Los Angeles, CA: Natural History Museum of Los Angeles County.

35. R Core Team. 2013 *R: a language and environment for statistical computing*. Vienna, Austria: R Foundation for Statistical Computing.

36. Schlager S. 2017 Morpho and Rvcg—shape analysis in R: R-packages for geometric morphometrics, shape analysis and surface manipulations. In *Statistical shape and deformation analysis* (eds G Zheng, S Li, G Székely), pp. 217–256. New York, NY: Academic Press.

37. Sokal RR, Michener CD. 1958 A statistical method of evaluating systematic relationships. *Univers. Kansas Sci. Bullet.* **28**, 1408.

38. Sustaita D. 2008 Muscoloskeletal underpinnings to differences in killing behavior between North American accipiters (Falconiformes: Accipitridae) and falcons (Falconidae). *J. Morphol.* **269**, 283–301. (doi:10.1002/jmor.10577)

39. Attard MRG, Wilson LAB, Worthy TH, Scofield P, Johnston P, Parr WCH, Wroe S. 2016 Moa diet fits the bill: virtual reconstruction incorporating mummified remains and prediction of biomechanical performance in avian giants. *Proc. R. Soc. B* **283**, 20152043. (doi:10.1098/rspb.2015.2043)

40. Moreno-Opo R, Trujillano A, Margalida A. 2020 Larger size and older age confer competitive advantage: dominance hierarchy within European vulture guild. *Sci. Rep.* **10**, 2430. (doi:10.1038/s41598-020-59387-4)

41. Purohit A, Saran R. 2013 Population status and feeding behavior of Cinereous Vulture (*Aegypus monachus*): dynamics and implications for the species conservation in and around Jodhpur.

42. Duriez O, Herman S, Sarrazin F. 2012 Intra-specific competition in foraging Griffon Vultures *Gyps fulvus*: 2. The influence of supplementary feeding management. *Bird Study* **59**, 193–206. (doi:10.1080/00063657.2012.658640)

43. Worthy TH, Holdaway N. 2002 *The lost world of the Moa: prehistoric life of New Zealand*. Bloomington, IN: Indiana University Press.

44. Bunce M et al. 2009 The evolutionary history of the extinct ratite moa and New Zealand Neogene paleogeography. *Proc. Natl Acad. Sci. USA* **106**, 20 646–20 651. (doi:10.1073/pnas.0906660106)

45. Brassey CA, Holdaway RN, Packham AG, Anné J, Manning PL, Sellers WI. 2013 More than one way of being a moa: differences in leg bone robustness map divergent evolutionary trajectories in Dinornithidae and Emeidae (Dinornithiformes). *PLoS ONE* **8**, e82668. (doi:10.1371/journal.pone.0082668)

46. Dickison MJ. 2007 Allometry of giant flightless birds. PhD thesis, Duke University.

47. Stettenheim PR. 2015 The integumentary morphology of modern birds—an overview1. *Am. Zool.* **40**, 461–477. (doi:10.1093/icb/40.4.461)

48. Duclos M, Sabat P, Newsome SD, Pavez EF, Galbán-Malagón C, Jaksic FM, Quirici V. 2020 Latitudinal patterns in the diet of Andean condor (*Vultur gryphus*) in Chile: contrasting environments influencing feeding behavior. *Sci. Total Environ.* **741**, 140220. (doi:10.1016/j.scitotenv.2020.140220)

49. Millien V. 2006 Morphological evolution is accelerated among island mammals. *PLoS Biol.* **4**, e321. (doi:10.1371/journal.pbio.0040321)

50. van Heteren AH et al. 2021 New Zealand's extinct giant raptor (*Hieraaetus moorei*) killed like an eagle, ate like a condor. Figshare.